Journal of Hydrology 577 (2019) 123997

Contents lists available at ScienceDirect

Journal of Hydrology

journal homepage: www.elsevier.com/locate/jhydrol

Research papers

Current travertines precipitation related to artificial CO_2 leakages from a natural reservoir (Gañuelas-Mazarrón Tertiary Basin, SE Spain)

Julio Rodrigo-Naharro[a,*], Maria J. Herrero[b], Antonio Delgado-Huertas[c], Arsenio Granados[c], Luis Pérez del Villar[a]

[a] Centro de Investigaciones Energéticas, Medioambientales y Tecnológicas (CIEMAT), Avda. Complutense 40, 28040 Madrid, Spain
[b] Dpto. de Petrología y Geoquímica, Facultad de Ciencias Geológicas, Universidad Complutense de Madrid, C/José Antonio Nováis 2, 28040 Madrid, Spain
[c] Laboratorio de Biogeoquímica de Isótopos Estables, Instituto Andaluz de Ciencias de la Tierra IACT (CSIC-UGR), Avda. de las Palmeras 4, 18100 Armilla, Granada, Spain

ARTICLE INFO

This manuscript was handled by P. Kitanidis, Editor-in-Chief, with the assistance of Andreas Hartmann, Associate Editor

Keywords:
CO_2 storage
CO_2 leakage
Travertines
Stable isotopes
Natural analogues
Betic Cordillera (Spain)

ABSTRACT

In the framework of a natural CO_2 reservoir with CO_2 leakages as an analogue of a failed CO_2 deep geological storage, the current precipitation of travertines and the associated upwelling of CO_2-rich saline groundwater were analysed. This natural analogue is located in the Gañuelas-Mazarrón Tertiary Basin (SE Spain). The study comprises of the chemistry of both groundwater and travertines, including stable isotopes, mineralogy and petrography of the travertines, all this performed after a review of the geology of the basin. In this sense, the basin gathers the main features of a safe natural CO_2 reservoir in a deep saline aquifer sealed by a thick marl formation. The aquifer was artificially perturbed by the drilling of wells, inducing the travertines precipitation at these water discharge points. Groundwater is saline, slightly acid, oversaturated in aragonite and calcite and with significant concentrations of heavy elements, some of them toxic. From an isotopic viewpoint, the relative constant δ^{13}C-DIC values suggest that carbon is mainly inorganic in origin with minor organic and mantle contributions. Travertines are basically composed of aragonite or calcite, their precipitation being controlled by a sudden CO_2 degassing and minor biological activity. Their δ^{13}C signatures indicate that carbon mainly has an inorganic origin, although some contribution of organic carbon must be considered as well. Furthermore, these carbonate deposits did not precipitate in isotopic equilibrium, as determined by δ^{18}O values. Finally, it is suggested that the appearance of travertines along with their carbon isotopic signatures represent efficient tools for detecting CO_2 leakages from any CO_2 storage site.

1. Introduction

Current continental carbonates occur in a wide variety of geological situations related to: pedogenic processes (soils, palaeosoils, calcretes); lacustrine and palustrine environments; karst caves (speleothems); and hot and cold springs (Herrero and Escavy, 2010). Travertines are formed where groundwater leaks to the surface, cools down, degasses resulting in the precipitation of these carbonate deposits. These rocks are usually composed of aragonite, calcite and sometimes dolomite, with a variety of crystal morphologies and chemical compositions. Numerous studies (Moore, 1956; Friedman, 1970; Folk, 1974, 1994; Pentecost and Viles, 1994; Farmer and Des Marais, 1994; Ford and Pedley, 1996; Guo and Riding, 1998, 1999; Frisia et al., 2000; Pentecost, 2005; Viles and Pentecost, 2007; Jones and Renault, 2010) have tried to establish the overriding variables controlling the precipitation of the different phases (i.e. temperature, growing inhibitors, water saturation index with respect to $CaCO_3$, CO_2 degassing rates and/or evaporation with the consequent increase in pH) as well as the influence of plants, algae and bacterial activity (photosynthesis/respiration). According to AGI (1962), the carbonate deposits within this study are considered as travertines, since they are surficial sedimentary rocks formed by the precipitation of carbonate minerals from solutions of hot springs. They are generally precipitated in response to physical CO_2 degassing and/or biochemical CO_2 consumption along streams and pools (Barnes, 1965; Guo and Riding, 1998).

Travertine deposits formed through leakages from natural CO_2 reservoirs have been described worldwide (e.g. Barnes et al., 1978; Pentecost, 1995; Jones and Renaut, 1996; Minissale et al., 2002; Liu et al., 2003; Moore et al., 2003; Shipton et al., 2004; D'Alessandro et al., 2007; Gibert et al., 2009; Uysal et al., 2009; Gal et al., 2011; Prado-

* Corresponding author.
E-mail address: julio.rodrigo@ciemat.es (J. Rodrigo-Naharro).

https://doi.org/10.1016/j.jhydrol.2019.123997
Received 11 January 2019; Received in revised form 28 June 2019; Accepted 26 July 2019
Available online 27 July 2019

Pérez and Pérez del Villar, 2011; Schütze et al., 2012; Burnside et al., 2013; Crespo et al., 2013; Prado-Pérez et al., 2013; Priewisch et al., 2013; Jones and Peng, 2016). These natural systems can be analogous to CO_2 Deep Geological Storages (CO_2-DGS) in deep saline and unusable aquifers. In this context, and through reasoning by analogy, the comprehensive study of these systems, including the CO_2 behaviour, can be useful to predict the long-term performance of a CO_2-DGS (Prado-Pérez and Pérez del Villar, 2011; Prado-Pérez et al., 2013). Consequently, fast travertine precipitation can be considered as clear evidence of CO_2 leakages from groundwater exhibiting a high CO_2 concentration.

In the framework of a large project on Carbon Capture and Storage (CCS) technologies, the Gañuelas-Mazarrón Tertiary Basin (GMTB), SE Spain, was studied as an analogue of a natural CO_2 reservoir affected by leakages (Pérez del Villar et al., 2008; Nisi et al., 2010a,b; Rodrigo-Naharro et al., 2011, 2012, Rodrigo-Naharro et al., 2013a,b; Rodrigo-Naharro, 2014; Rodrigo-Naharro et al., 2017, 2018). CO_2-rich saline groundwater from deep and thermal aquifers are currently upwelling through geothermal wells, precipitating travertines at the water discharge points.

In order to establish the different analogies between the GMTB and a CO_2-DGS, the following analyses were performed: (i) a general review of the main geological and hydrogeological features of the GMTB; (ii) the relationships between groundwater and the actively forming travertine deposits; and (iii) the establishment of the main factors that induce their precipitation. The results of the present study comprise a dataset of groundwater chemistry, including stable isotopes ($\delta^{18}O$, $\delta^{2}H$, $\delta^{13}C$-DIC). Additionally, the mineralogy and petrography of the carbonate deposits and their stable isotope signatures ($\delta^{13}C$, $\delta^{18}O$) were also determined.

This work aims to: (a) study the physicochemical and isotopic features of the carbonates precipitated from CO_2-rich waters in the GMTB; (b) better understand the main processes involved in the formation of travertines related to artificial CO_2 leakages from natural or artificial CO_2 reservoirs; (c) use this information for tracking the CO_2 source; and (d) establish the analogies between a natural CO_2 reservoir and a CO_2-DGS affected by leakages derived from anthropogenic activities. Furthermore, it has assisted with the identification of the cause of precipitation of the different calcium carbonate phases.

2. Geological background

The GMTB is located in the SE of the Iberian Peninsula, in the eastern Betic Cordillera, within the Internal Zone. It is a subsidiary basin, but tectonically related to the Guadalentín River Basin. It is delimited by extensional faults and Neogene volcanic rocks and formed by a metamorphic basement composed of the Nevado-Filábride and the Alpujárride Complexes (Fig. 1). The first Complex belongs to the Permo-Triassic sequence consisting of schists, quartzites, gneisses, marbles and limestones with interbedded gypsum. The second comprises schists, slates, quartzites, salts, conglomerates and sandstones of Permian age, as well as Triassic limestones and dolostones (Cerón et al., 1998, 2000). Almost all of these geological complexes outcrop in the reliefs that delimit the basin, which is filled by a thick Neogene sedimentary formation consisting of a succession of sandy marls and calc-marls, conglomerates, limestones, sandstones, calc-sandstones, with gypsum and other sulphates, such as barite and celestite. This last characteristic is common in all of the Tertiary intramontane sedimentary basins from the Betic Cordillera (Sanz de Galdeano and Vera, 1992). These sediments were intruded by Neogene volcanic materials such as andesites, dacites and rhyodacites, particularly located in the faulted boundaries of the basin (Barragán, 1997). Rhyodacites are U-rich with an average concentration of 14 ppm of U, occurring mainly as microcrystals of uraninite (UO_2) included within zircon crystals (Rodrigo-Naharro et al., 2012; Rodrigo-Naharro, 2014). The aforementioned sedimentary and volcanic materials are covered by Plio-Quaternary sediments consisting of conglomerates, sands, silts and argillites.

The geophysical studies performed within this basin by Rodrigo-Naharro et al. (2018) confirm the existence at depth of the above-mentioned three primary groups of geological materials. Evidence of these has been supported through differences in resistivity logs: the Nevado-Filábride Complex, the Tertiary sedimentary succession and the more or less altered Neogene volcanic rocks that normally intrude into the sedimentary materials. Regarding the morphology, the GMTB is a graben structure limited by the Nevado-Filábride materials affected by vertical faults with significant downthrows and frequently filled by volcanic rocks. The modelled cross section A-A' (see Figs. 1 and 2a) obtained from a gravimetric research study shows a geological model of the GMTB with its vertical boundaries and a deeply sunken central zone (~9 km wide) divided into two sectors, reaching a depth of about 900 m in the SW sector (Rodrigo-Naharro et al., 2018). This geological model (see Fig. 2a) is complimented by the El Saladillo lithostratigraphc column (Fig. 2b), which was obtained from a detailed analysis of drill-cuttings. It has been used to develop the model of the A-A' gravimetric cross section.

From a hydrogeological point of view, the GMTB has numerous aquifers but with small extent, all of them belonging to the Mazarrón Hydrogeological Unit (MHU) (Fig. 3). Amongst these, five main aquifers were recognised in the basin: La Ermita de El Saladillo, Gañuelas, La Majada, La Majada-Leyva and Las Moreras (IGME, 1981; Navarro et al., 1993). The Totana aquifer was also recognised, and forms part of the Bajo Guadalentín Hydrogeological Unit. This aquifer (~120 km^2), located in the NW border of the GMTB (see Fig. 3), lies within lenticular detrital layers, more or less hydraulically connected, and intercalated in the Tertiary marly formation filling the Guadalentín basin.

The hydrogeology of the region is mainly characterised by these facts: (i) the areas of recharge are practically confined to the Permo-Triassic reliefs and, to a lesser extent, to discontinuous detrital levels that crop up in the Tertiary basins; (ii) the limited volume of rainfall hampers the recharge of the aquifers; (iii) the existence of confined aquifers with little extent, emplaced within the Permo-Triassic materials and/or in the Tertiary volcanic materials, characterised by their high salinity and CO_2 oversaturation; (iv) the existence of smaller shallow lying aquifers within the Neogene permeable materials filling the Tertiary basins, which although well confined have less saline water; (v) the existence of a thick Neogene marly formation that act as a seal for the deepest aquifers of the Tertiary basins of the region, such as the Guadalentín Basin and the studied basin; and (vi) the decrease in the piezometric level of the shallow aquifers due to their over-exploitation, which has caused them to become contaminated from the deepest, saline and CO_2-enriched aquifers. As regards the GMTB, this basin is characterised by the existence of numerous groundwater wells drilled in the 1960 s for agricultural purposes, whose depths range from between 100 and 300 m. The continuous groundwater overexploitation resulted in a consequent drop of the water table and pressure, causing the uprising of saline CO_2-rich groundwater from depth and located in the contact between the Nevado-Filábride Complex and the Neogene sedimentary materials (Cerón et al., 1998, 2000). The analysis of the piezometric data of the main aquifers of the MHU shows a general decline in the piezometric levels from the beginning of 1980s and a period of stabilization from the second half of that decade, probably due to the fact that they were abandoned (CHS, 2005).

The waters and carbonates studied here belong to La Ermita de El Saladillo and Gañuelas aquifers since they are the only ones in which carbonate deposits are currently being precipitated. The main hydrogeological characteristics of these aquifers, summarised in Table 1, are as follows:

1) La Ermita de El Saladillo is hosted in the Nevado-Filábride marble formation and Neogene volcanic rocks, both being hydraulically connected. Its internal structure is like a graben, laterally limited by

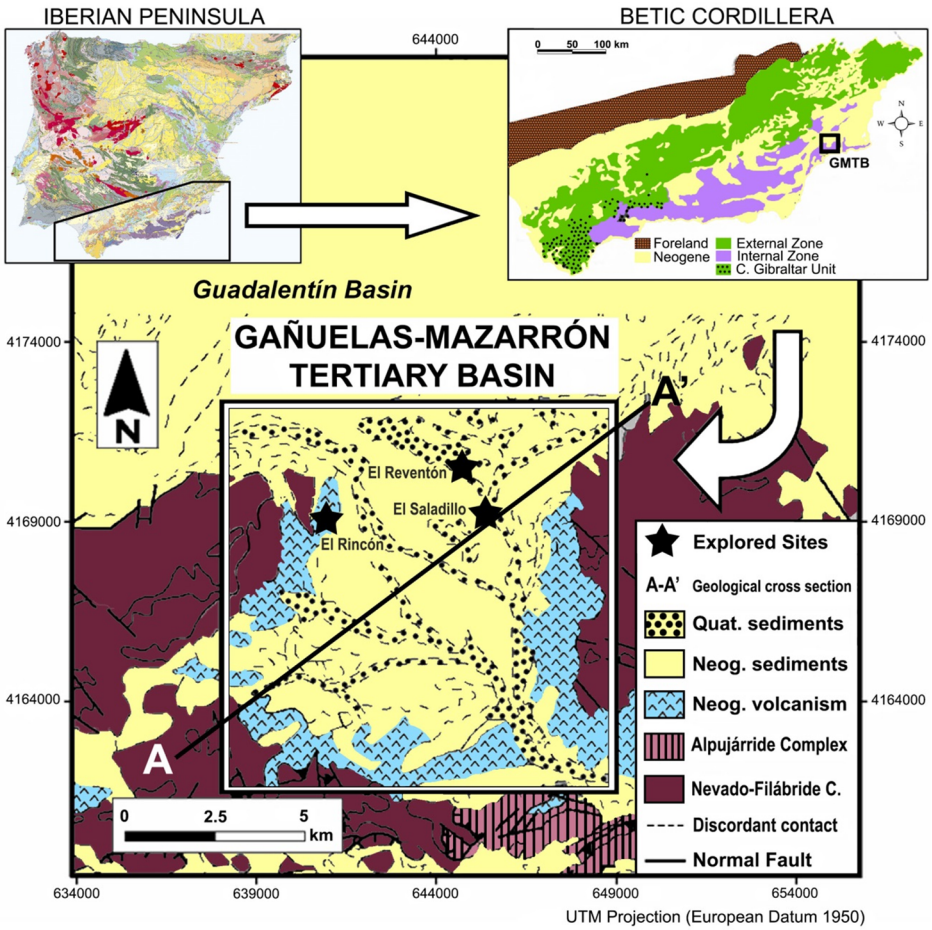

Fig. 1. Schematic geological map of the Gañuelas-Mazarrón Tertiary Basin, in South-Eastern Spain.

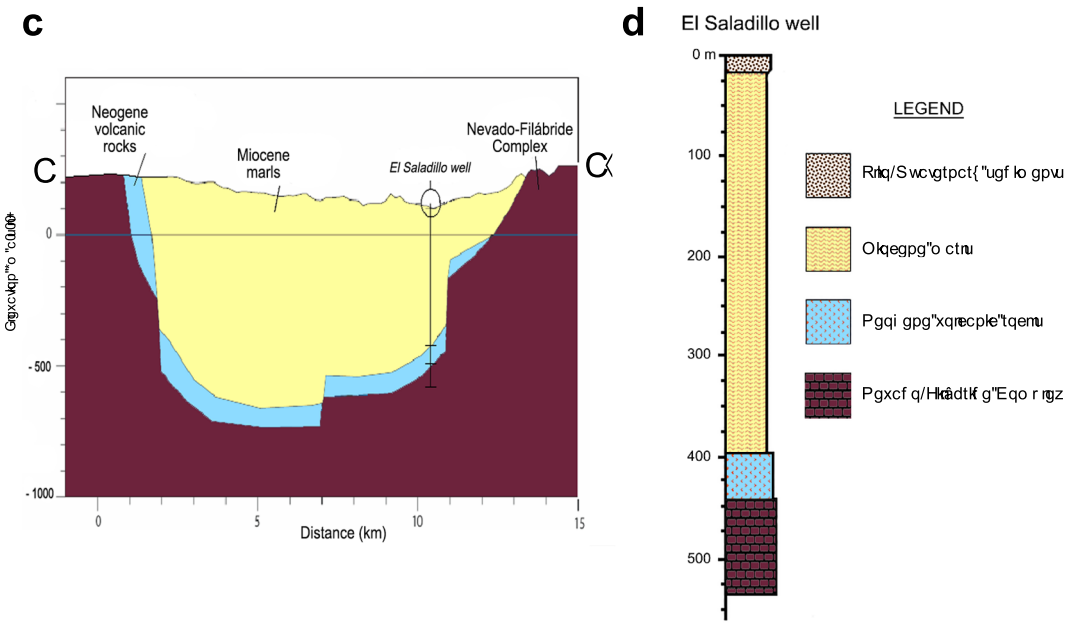

Fig. 2. (a) Geological interpretation of the gravimetric profile A-A'. (b) Lithostratigraphic column from El Saladillo well (IGME-ADARO, 1985, modified).

the outcrops of the Neogene volcanic rocks that, in turn, constitute the seal of the aquifer. It has an area of ~46 km^2 and was intersected by the El Saladillo and El Reventón wells (see Fig. 3).

2) Gañuelas is also emplaced in the Nevado-Filábride formation and extends for about 4 km^2, being intersected by the El Rincón well. This aquifer is located above the impermeable substrate formed by the Permo-Triassic materials of the Alpujárride Complex (see Fig. 3).

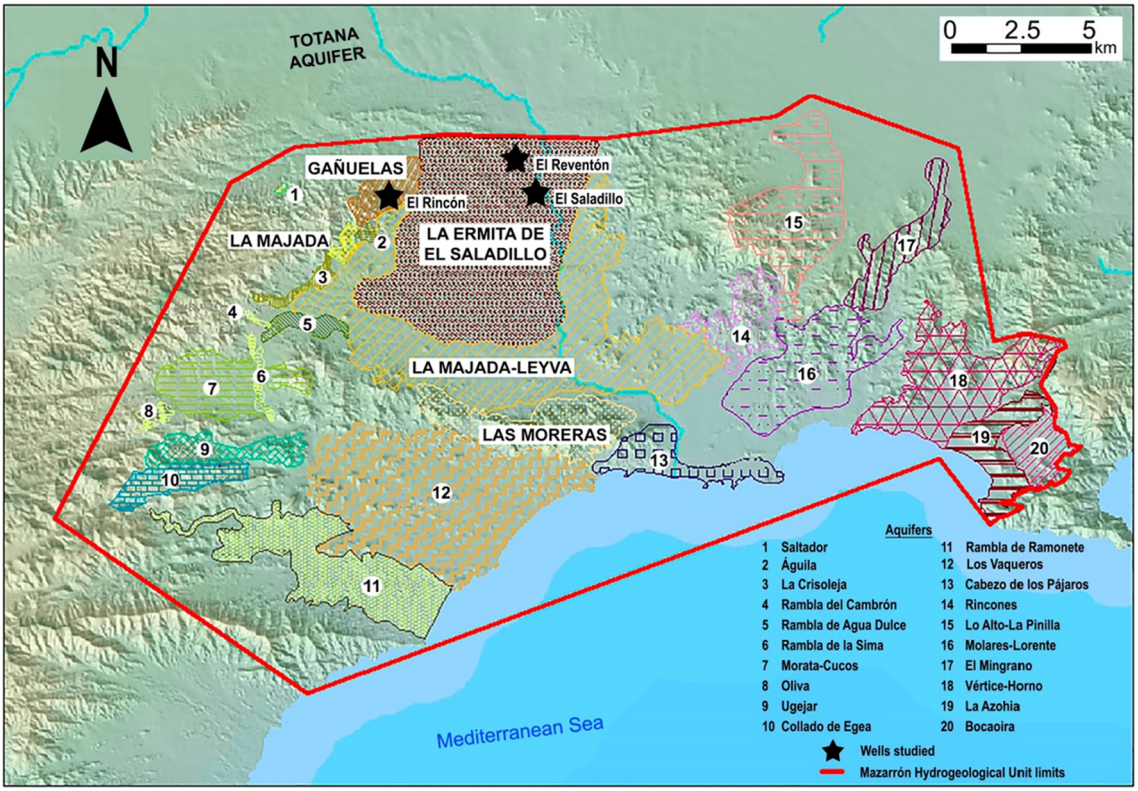

Fig. 3. Limits of the Mazarrón Hydrogeological Unit, where the five main aquifers are located. Note that the La Ermita de El Saladillo aquifer practically overlaps in extension to the Gañuelas-Mazarron Tertiary Basin.

3. Materials and methods

3.1. Groundwater

A total of 4 groundwater samples were taken at the wellhead from each of the 3 wells considered (El Saladillo, El Reventón and El Rincón). These samples were collected between 2010 and 2011 during the spring and summer. Afterwards they were stored at 4 °C prior to their analysis which was performed at room temperature.

For each water sample, two plastic vials were utilised to collect 1 L and 100 mL samples for anion and cation analyses, respectively. The pH values were measured *in situ* at the wellhead using a pH-meter, consisting of a voltmeter, a pH electrode and a temperature probe, with automatic compensation and accuracy to 0.1 °C. It was calibrated by recording the electrical signal obtained by measuring the pH of two standard solutions, buffered to pH 4 and 7, at temperatures between 25 and 35 °C similar to those of the samples. The electrical conductivity (EC) was also measured *in situ* by a conductivity-meter with a K = 1 cell and automatic temperature compensation in the range between 10 and 70 °C. In addition, *in situ* total alkalinity in each sample was also determined, following the UNE-EN ISO 9963-1 standard and the 2320 method, which is conveniently described in "Standard Methods for the Examination of Water and Wastewater". The Redox potential meter (Eh) was measured *in situ* at the wellhead as well, by using a voltmeter with a microprocessor, an electrode of Pt-Ag-ClAg and a temperature probe. For Eh measurements, no calibration takes place, only a check to confirm that the equipment is measuring correctly. For this, the accuracy and reproducibility of the measurements made in several buffer solutions of known Eh is usually checked. All these measurements (pH, EC, Eh) were performed by using a multi-parameter handheld meter (Multi 350i, WTW, Weilheim, Germany).

Anion determination was undertaken at the University of Zaragoza, almost immediately after sampling. The Cl and F contents were determined by direct potentiometric measurement. Total dissolved sulphates were indirectly determined by molecular absorption spectrometry, according to the Nemeth (1963) method, and PO_4^{3-} contents were obtained by spectrophotometry.

Cations analyses (Ca, Na, Mg, K, Fe, Mn) were obtained by Atomic Absorption Spectrometry (AAS), while Al_2O_3 and SiO_2 were measured by Graphite Furnace Atomic Absorption Spectrometry (GFAAS) and Inductively Coupled Plasma-Optical Emission (ICP-OES), respectively. Trace elements (Sr, Li, As, Mn, Se, Cr, U, Ba, Be, Th, Tl, Co, Mo, Ni, Sb, V, Zn, Cu, Pb) were determined by Inductively Coupled Plasma-Mass Spectrometry (ICP-MS). These analyses were performed in the CIEMAT (Centro de Investigaciones Energéticas, Medioambientales y Tecnológicas) laboratories.

The charge-balance error for each sample, using the PHREEQC code (Parkhurst and Appelo, 2013) and WATEQ4F thermodynamic database (Ball and Nordstrom, 2001), was calculated as part of an analysis quality test. In this sense, a charge-balance error of less than about 5% was considered to be acceptable (Appelo and Postma, 2005), although this error can be higher particularly in very dilute or saline solutions

Table 1
Main hydrogeological features of the two studied aquifers (IGME, 1979; Navarro et al., 1993).

Aquifer	Area (km^2)	Host-rock lithology	Host lithology age	Thickness (m)	Water table depth (m)	Wells
La Ermita de El Saladillo	~46	Marbles and volcanic rocks	Triassic and Miocene	60–90	441–617	El Saladillo El Reventón
Gañuelas	~4	Marbles	Triassic	200	200	El Rincón

Table 2
Chemistry of groundwater from which carbonate deposits precipitate.

Physicochemical parameters	El Saladillo		El Reventón		El Rincón	
	Mean value	Std. Dev.	Mean value	Std. Dev.	Mean value	Std. Dev.
T (°C)	45.6	0.4	45.7	0.2	35.9	0.6
EC (μS/cm)	9388	1101	8905	1322	5385	433
pH	6.8	0.1	6.5	0.0	6.4	0.0
Eh (mV)	−46	—	−268	—	51	—
Major elements (mg/L)						
HCO_3	2009	36	1993	31	2159	125
SO_4	3529	175	3458	305	1775	190
Cl	1129	31	1050	19	203	6
PO_4	25.3	7.0	24.1	6.6	23.5	1.3
F	2.9	0.1	2.6	0.1	1.4	0.04
Ca	554	48	452	55	355	76
Mg	251	23	205	35	121	22
Na	2354	350	2250	172	1177	136
K	84	9	76	7	35	2
Fe_{total}	3.83	1.1	2.38	6.3	1.13	2.6
SiO_2	16.6	2.5	16.4	1.4	13.0	1.5
Mg/Ca ratio	0.45	0.48	0.45	0.64	0.34	0.29
Trace elements (μg/L)						
Sr	8100	5381	3131	1769	2760	2293
Li	2886	212	2934	204	1008	106
As	37.1	17.2	24.1	3.5	15.5	0.4
Mn	41.5	20.1	36.1	17.5	22.0	3.6
Se	13.4	10.1	10.4	6.9	10.5	0.0
Cr	36.2	24.2	35.1	19.8	12.6	3.5
U	4.3	0.6	3.4	0.3	11.5	1.3
Ba	8.2	1.9	18.3	2.2	14.9	1.4
Be	1.9	0.3	1.6	0.1	0.5	0.1
Th	0.1	0.1	0.1	0.2	0.1	0.1
Tl	0.2	0.03	0.01	0.01	0.3	0.05
Al	81.6	0.0	62	60.6	226	0.0
Co	1.0	0.1	0.4	0.0	0.5	0.1
Mo	1.2	0.2	1.3	0.3	1.0	0.2
Ni	14.0	3.2	7.7	5.2	12.2	3.7
Sb	0.2	0.1	0.1	0.0	0.3	0.2
V	13.7	4.8	12.9	4.1	2.6	0.6
Zn	21.7	7.4	10.7	9.6	30.6	4.1
Cu	13.0	2.1	14.0	2.7	10.2	1.8
b	0.3	0.3	0.1	0.1	0.4	0.2
Isotopic signatures(‰)						
$\delta^{18}O_{(V\text{-}SMOW)}$	−6.9	0.2	−6.3	0.3	−6.9	0.1
$\delta^{2}H_{(V\text{-}SMOW)}$	−39.5	6.7	−34.7	5.0	−38.8	2.2
$\delta^{13}C_{(V\text{-}PDB)}$	−5.6	2.1	−6.4	1.8	−6.4	0.9
Charge balance error (%)	8.5		2.1		1.3	
Hydrochemical classification	Na-Ca-SO_4		Na-Ca-SO_4		Na-Ca-SO_4-HCO_3	
Saturation Index (SI)	Calcite (0.96); aragonite (0.83)		Calcite (0.62); aragonite (0.49)		Calcite (0.44); aragonite (0.30)	

(Zhu and Anderson, 2002).

Piper-Hill diagrams were used for the classification of water through the INAQUAS code (Moreno and De la Losa, 2008). Speciation-solubility calculations were performed using the PHREEQC code as well as the WATEQ4F thermodynamic database.

Finally, a cluster analysis (dendrogram) was performed to illustrate the grouping of samples from the aquifers belonging to the GMTB, also including the Totana aquifer. For that, 18 representative samples were selected and temperature, pH, major elements, EC and alkalinity were considered as variables.

3.2. Travertine deposits

Carbonate deposits currently forming at the groundwater upwelling points of the 3 wells considered in this study were collected in springs during 2010 and 2011.

The mineralogical composition of the travertines was obtained by X-Ray Diffraction (XRD) and Differential Thermal and ThermoGravimetric analyses (DTA + TG). The XRD analysis was performed by using the non-orientated powder method on ground up, sieved and homogenised < 60 μm sized samples. The mineral phases were identified comparing the experimental reflections spacing with those from the "Index X-Ray data for minerals (JCPD)" database.

Petrographic characterisation was performed by Optical Microscope (OM). This technique allows the identification of the major and accessory minerals and identifies the main textural features, which were illustrated by photomicrographs. Besides this, these characteristics were complemented by Backscattered Electron Images (BEI) performed by Scanning Electron Microscopy (SEM) coupled to an Energy Dispersive X-ray spectrometer (EDX).

Chemical analyses of the bulk samples were performed in the CIEMAT laboratories. Cation analyses (Ca, Na, Mg, K, Fe, Mn) were determined by Inductively Coupled Plasma Optical Emission Spectrometry (ICP-OES), while Na and K were determined by Flame Atomic Emission Spectroscopy (FAES). Trace elements, except U, Th and Zr, were determined by Inductively Coupled Plasma Mass Spectrometer (ICP-MS). Uranium was determined by Laser Induced Kinetic Phosphorimetry, whilst Th and Zr were measured on powder samples by X-Ray Fluorescence (XRF). An elemental analyser was used for total C and S determinations.

3.3. Stable isotopes

$\delta^{18}O$, $\delta^{2}H$ and $\delta^{13}C$-DIC isotopic ratios were measured in the laboratory for the groundwater samples. The $\delta^{18}O$ signature in water was analysed using the CO_2-H_2O equilibration method (Cohn and Urey, 1938; Epstein and Mayeda, 1953). For $\delta^{2}H$ analysis, an aliquot of water (0.5 μL) was injected into a ceramic column containing a glassy carbon tube at 1450 °C, producing H_2 and CO gases (Sharp et al., 2001). The H_2 was separated out by chromatography using a He carrier stream connected online with a Pyrolysis Furnace TC/EA and analysed in a mass spectrometer. The experimental error in the determinations of $\delta^{18}O$ and $\delta^{2}H$ was < 0.15 and 2‰, respectively. Before the $\delta^{13}C$-DIC analyses, water samples were filtered (0.45 μm) *in situ* by means of a syringe into 12 mL vials, followed by poisoning with $HgCl_2$ in order to avoid secondary biological activity. They were then capped, leaving no headspace, and stored at 4 °C before analyses. The CO_2 was then separated from other residual gases by chromatography. The analyses were performed at room temperature in a thermostatic bath.

For the carbonate deposits, $\delta^{13}C$ and $\delta^{18}O$ isotopic values were determined using a < 60 μm sized sample aliquot, with an experimental error of < 0.1‰. Isotopic ratios were normalised with respect to the fractionation factors (α): 1.01044 for calcite (Kim and ÓNeil, 1997), and 1.01034 for aragonite (Kim et al., 2007), both at 25 °C. All the isotopic results were reported in the standard delta notation (δ ‰) relative to the international V-SMOW and V-PDB standards. Samples were stored at room temperature, whilst the analyses were performed in a thermostatic bath at 50 °C. All isotope ratios were obtained at the laboratories of Instituto Andaluz de Ciencias de la Tierra (CSIC-UGR, Granada).

4. Results

4.1. Groundwater

The main physicochemical features of the 4 measurements of each groundwater from the 3 sampled wells, reported as the mean value with the standard deviation (Table 2) indicate that: (i) El Rincón water is warm (20–40 °C) whilst El Saladillo and El Reventón are mesothermal (40–75 °C) waters (Pentecost, 2005); and (ii) they are brackish since EC values vary from 5385 (El Rincón) to 9388 μS/cm (El Saladillo); slightly acid, with pH values ranging from 6.4 (El Rincón) to 6.8 (El Saladillo); and either weakly reduced, since Eh values range from −268 mV (El

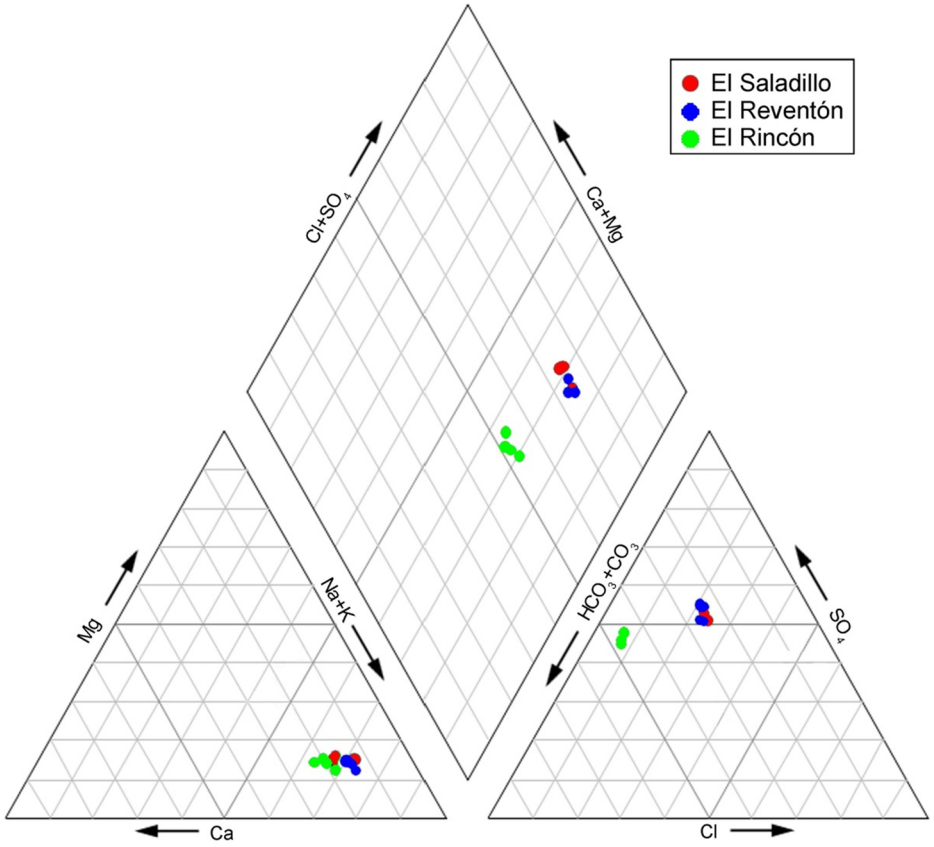

Fig. 4. Piper-Hill diagrams where the studied groundwater is plotted.

Reventón) to −46 mV (El Saladillo), or slightly oxidised (El Rincón: 51 mV). The high bicarbonate concentration of the waters is confirmed by the pH values. Major ions allow the classification of El Saladillo and El Reventón as Na-Ca-SO_4 waters, whereas El Rincón water is Na-Ca-SO_4-HCO_3 (Fig. 4). The charge-balance errors were considered to be acceptable, including El Saladillo water although it has a high salinity (see Table 2).

Concerning heavy elements, concentrations of Fe, As, Mn and Al exceed the drinking water standards and health advisories established by the U.S. Environmental Protection Agency (USEPA, 2012). It is worth noting the high concentration of Fe.

Saturation Indices (SI) show that groundwater appears oversaturated with respect to calcite and aragonite, specially El Saladillo and El Reventón (see Table 2), which have values much higher than the uncertainty degree, established in ± 0.35 (Plummer and Busenberg, 1982; Deutsch et al., 1982; Back et al., 1983; Nordstrom and Ball, 1989; Tena et al., 1990).

Regarding stable isotopes, $\delta^{18}O$ and $\delta^{2}H$ values of groundwater (see Table 2) were plotted in relation to the Global Meteoric Water Line as defined by Craig (1961) (GMWL: $\delta^{2}H = 8 \times \delta^{18}O + 10$) and the Mediterranean Meteoric Water Line (MMWL: $\delta^{2}H = 8 \times \delta^{18}O + 22$) as defined by Gat and Carmi (1970, 1987) (Fig. 5). Accordingly, all samples, located above the GMWL, are ^{2}H-enriched, similar to the values of the meteoric waters from SE Spain (Cerón et al., 1998; Delgado and Reyes, 2004; Araguas-Araguas and Díaz-Teijeiro, 2005). $\delta^{13}C$-DIC values are relatively constant, varying from −6.4‰ (El Reventón and El Rincón) to −5.6‰ (El Saladillo).

Finally, the dendrogram constructed from samples belonging to the GMTB and the Totana aquifer (Fig. 6) shows two clusters. Cluster C-1 groups the vast majority of the samples belonging to the different aquifers, except those belonging to La Ermita de El Saladillo, Gañuelas and Totana, which are clustered in turn in C-2. These samples are characterised because they are brackish with high EC values. The distance between clusters C-1 and C-2 is high enough to not be able to establish any relationship between them.

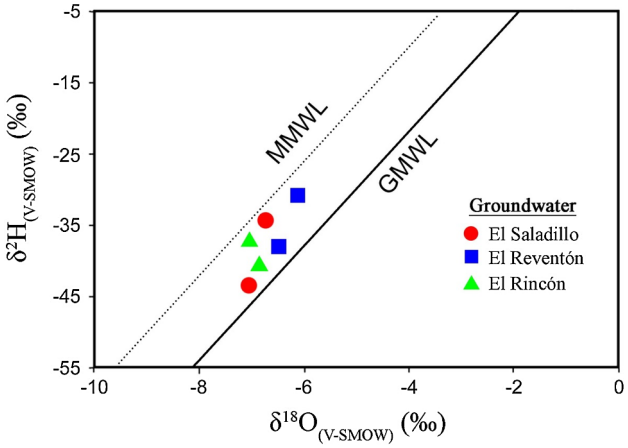

Fig. 5. Representation of the $\delta^{18}O$ and $\delta^{2}H$ values of groundwater in relation to the Global Meteoric Water Line (GMWL) as defined by Craig (1961) and the Mediterranean Meteoric Water Line (MMWL) as defined by Gat and Carmi (1970, 1987).

4.2. Travertine deposits

The El Saladillo sample corresponds to a travertine deposit formed by vertical accretion at the air–water interface. Water comes out through the pipeline, falling into a pool and splashing on its walls (Fig. 7a and b). This water precipitates carbonates forming micro-terraces (Fig. 7c) composed of mm-thick carbonate laminae with a

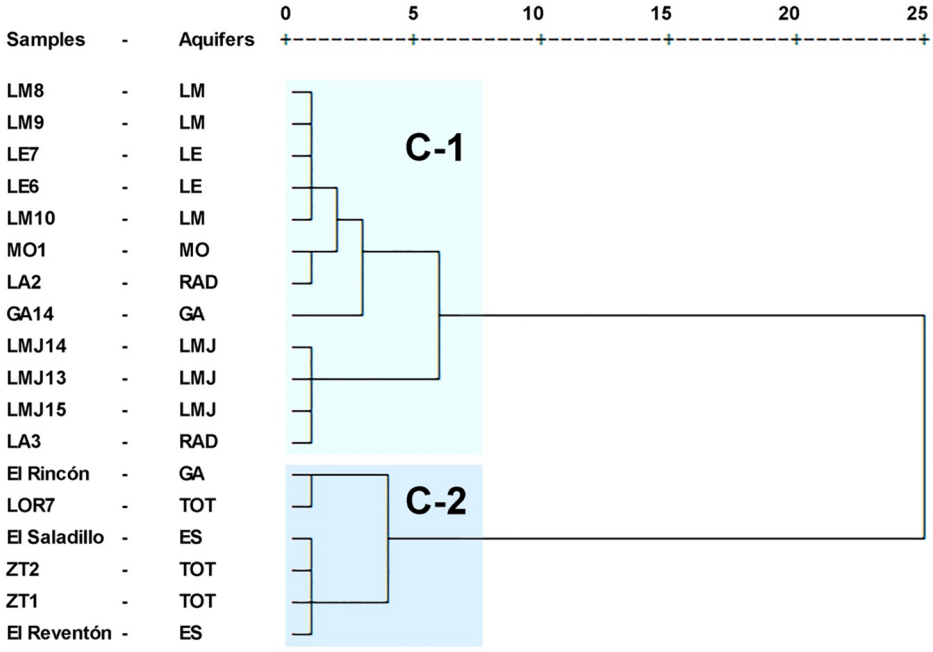

Fig. 6. Dendrogram performed from 18 representative samples from the aquifers belonging to the GMTB and the Totana aquifer. The figure shows two clusters (C-1 and C-2) that group the samples with similar chemical and physico-chemical characteristics. (GA = Gañuelas; RAD = Rambla de Agua Dulce; LM = Las Moreras; LE = La Majada-Leyva; LMJ = La Majada; MO = Morata-Cucos; ES = La Ermita de El Saladillo; TOT = Totana).

stromatolite-like structure (Fig. 7d). The precipitation rate was established to be ~5 mm/month.

The El Reventón sample was taken from the interior of a water pipeline that belongs to a thermal spa facility (Fig. 7e), whereas the El Rincón sample forms a thin carbonate crust produced as a result of a water-drop leakage from the pipeline of a hydrological well (Fig. 7f).

The semi-quantitative mineralogical composition of the carbonate samples show that aragonite and calcite constitute the main minerals (Table 3). Dolomite, goethite and quartz were also detected in some of these samples.

Furthermore, the same travertine samples analysed mineralogically have also been petrographically characterised using OM.

The travertine sample from El Saladillo was formed as a carbonate crust that has a stratiform stromatolite-like fabric. It contains abundant calcified bubbles which appear encrusted by micrite. The sample is composed of a repetitive alternation of silt-sized micritic aggregates layers (1 μm thick that varies in thickness laterally) that have been partially recrystallised to sparite. It also shows abundant shrub-like morphologies (Fig. 8a). The shrubs are upward radiating "branches" that are composed of chains and groups of leaves which are micritic accumulations around bacterial clumps. The shrubs nucleate on top of a substrate and growth perpendicularly. Between the shrubs appears abundant porosity which is encrusted by needles (Fig. 8b) of aragonite (10–100 μm of diameter), as determined by XRD. These needles of aragonite are < 1 μm wide and 200 μm long, and form spherulites (Guo and Riding, 1998; Pentecost, 2005) that correspond to bacterial clumps, that in some cases can rapidly be inverted to calcite.

The El Reventón sample is also composed of a stratiform stromatolite-like fabric constituted by an alternation of laminae of filamentous cyanobacteria such as *Phormidium*-like microbes (Fig. 8c), which are typical of travertine deposits formed within waters with temperatures cooler than 65 °C. Similarly to the El Saladillo sample, aragonite precipitates on and around the filamentous microbes, appearing as if they initiated growth vertically on micrite-aggregates layers, which are 1 μm thick. There are abundant pore spaces that are interpreted as the former sites of bacteria (Fig. 8d).

The El Rincón sample forms as microterracetes with abundant plant material (Fig. 8e) that has been covered by Ca-carbonates showing a very similar fabric to previous samples, although XRD analyses reveal that the only carbonate phase is calcite. Moreover, this sample also shows concentric micrite layers around different nuclei forming bacterial oncoids (Chafetz and Meredith, 1983; Folk and Chafetz, 1983). The different layers of micrite appear partially recrystallized to sparite, although the micrite aggregates are dominant. The topmost part of the sample, which represents the latest deposit (Fig. 8f), consists of alternating laterally continuous laminae of micritic aggregates with a stromatolite-like structure, with abundant porosity. As in the El Saladillo sample, these structures represent successive bacterial clumps, firstly living in terrace pools until laminated shrub-like structures are produced (Renault and Jones, 2000).

The compactness of the El Saladillo and El Reventón samples allows the determination of their minor and accessory minerals on polished thin sections by using SEM + EDX. Among them, botroydal Fe-oxyhydroxides, like goethite, are highlighted (Fig. 9a). Moreover, probably detrital, idiomorphic and partially altered pyrite (Fig. 9b), as well as early diagenetic framboidal pyrite, either oxidised or not, were also detected, indicating probable organic matter activity (Crespo et al., 2013; Rodrigo-Naharro et al., 2013b; Rodrigo-Naharro, 2014) and variations from reduced to oxidised conditions just after its formation (Fig. 9c and d). Iron carbonate and probably ankerite were identified within the carbonate mass, as well as celestite, barite and sphalerite.

The chemical composition (major, minor and trace elements) of the carbonate deposits is summarised in Table 4. Setting aside the high content in CaO and inorganic CO_2, the most relevant oxides are: (i) Fe_2O_3 in El Saladillo and El Reventón; (ii) SO_3 in all samples; and (iii) organic CO_2. Regarding trace elements: Ba, Sr, As, Zn, U, Ce, La and Zr concentrations are significant in some of the samples. The isotopic signatures of C ($\delta^{13}C$) show similar average values in the range between −1.8‰ and −0.7‰. With respect to $\delta^{18}O$ values, El Saladillo has −11.2‰, whilst El Reventón and El Rincón have −8.8‰ and −7.9‰, respectively (see Table 4).

5. Discussion

5.1. Groundwater

From the groundwater chemistry, it can be stated that El Saladillo and El Reventón are mesothermal (Pentecost, 2005) and sourced from the same aquifer (La Ermita de El Saladillo). However, El Rincón groundwater (Gañuelas aquifer) is warm and shows differences with

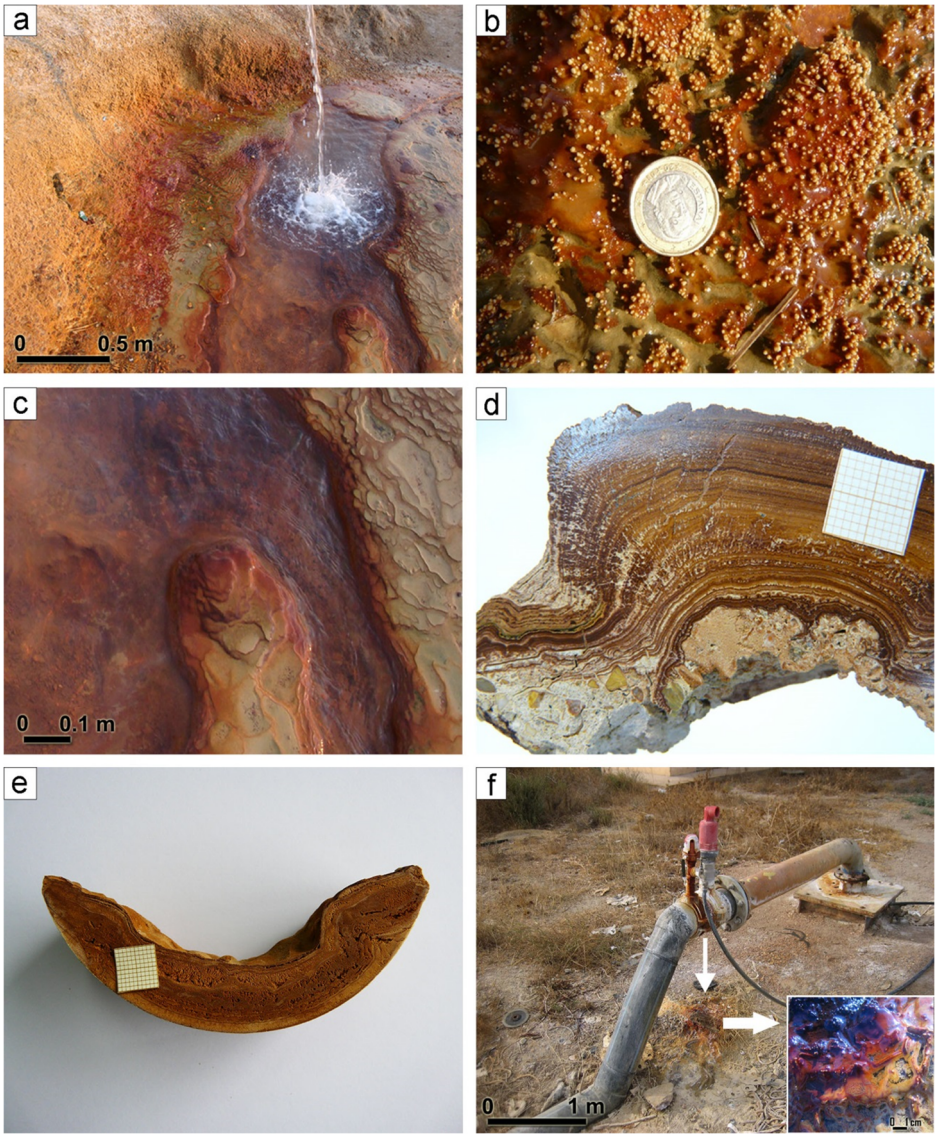

Fig. 7. (a) Travertine deposits formed from El Saladillo groundwater, where a sample was collected. (b) Travertine precipitation resulting from the splashing of groundwater. (c) Travertine deposits forming micro-terraces. (d) Detail of these travertine deposits composed of mm-thick carbonate laminae with stromatolite-like structure as well. (e) Travertine collected from the fillings of the thermal water pipelines of El Reventón. (f) El Rincón well facility where a water leakage is forming a very small reddish travertine deposit.

Table 3
Semi-quantitative mineralogical composition of the carbonate deposits obtained by XRD, expressed in % v/v.

Samples	Aragonite	Calcite	Dolomite	Goethite	Quartz	Total
El Saladillo	86	3	3	8	–	100
El Reventón	89	5	–	6	–	100
El Rincón	–	96	–	–	4	100

respect to the previous groundwater in relation to its Cl and SO_4 contents.

The dissolution of CO_2 in groundwater is responsible for the slightly low pH (6.4–6.8), whilst Eh values indicate variable redox potential at the surface, ranging from −268 mV (El Reventón) to 51 mV (El Rincón), suggesting that groundwater should be more reducing at depth. In this sense, the fast ascent of groundwater, particularly in El Saladillo and El Reventón artesian wells, is enough to preserve their reduced character even under oxidising atmospheric conditions. High salinity and redox parameters of some groundwater, particularly from the La Ermita de El Saladillo aquifer, could be explained due to the high residence times. In general, groundwater from the GMTB shows high salinity similar to the Guadalentín Basin, as this salinity is the result of a mixture of groundwater flowing through salts-rich Miocene rocks and infiltrating meteoric water, which also dissolves salts (Cerón and Pulido-Bosch, 1996; Martín-Vallejo, 1997; Cerón et al., 2000). Moreover, groundwater from both basins are also CO_2-enriched, as occurs in groundwater from active seismic and volcanic areas worldwide (Barnes et al., 1978; Jones and Peng, 2016).

Concerning Fe and trace elements, they can be sourced either from the marbles of the Nevado-Filábride Complex that host exploitable ore-deposits (Torres-Ruiz, 1980) or from the dissolution of the sulphide ore-deposits associated with the Neogene volcanism in the GMTB (Cerón et al., 2000). This last process could also explain the high content of As and Mn in these groundwaters, making them non-potable water. Nevertheless, As could also result from agricultural pollution due to the use of herbicides, pesticides or even fertilizers based on superphosphate (Fetter, 1993). Concerning the other trace elements, it is possible to highlight the following aspects: (i) the high Sr and Li contents are

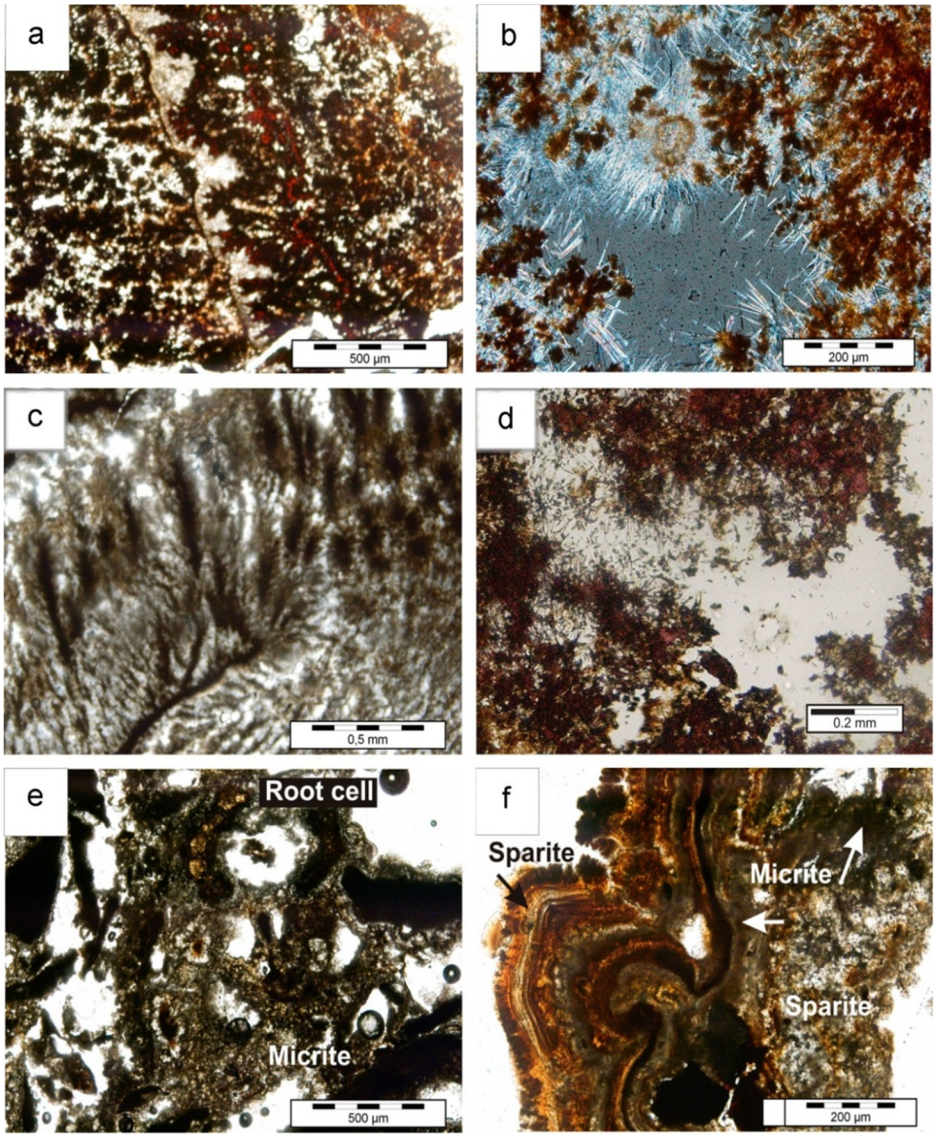

Fig. 8. Photomicrographs of samples: El Saladillo (a) (b); El Reventón (c) (d); and El Rincón (f) (g). (a) Shrubs with upward radiating "branches" that are composed of chains and groups of leaves which are micritic accumulations around bacterial clumps. (b) Aragonite needles growing from a micritic bacterial clump. (c) Calcite layers (bacterial clumps) with branches and high porosity. (d) Detail of this porosity partially filled by aragonite needles. (e) Micritic microbial clumps, partial dissolution of some of them; abundant plant material and even root cells. (f) Stromatolite-like fabric composed of an alternation of micrite and sparite lamination and nucleus formed by bacterial clumps.

related to the carbonate rocks that compose the basin basement (Gómez-Pugnaire et al., 1981) and to the dissolution of marine salts, respectively; (ii) the relatively high Cr concentrations, particularly in El Saladillo and El Reventón, are probably associated with the corrosion of the water distribution pipelines, a process that may also be partially responsible for the Fe and Mn values; (iii) the relevant U concentrations are probably related to the dissolution of uraninite (UO_2) from the U-rich volcanic rocks existing in the basin (Rodrigo-Naharro et al., 2012, 2017). In summary, it can be argued that the slightly acid groundwater studied has a great capacity to dissolve and transport a large amount of heavy elements towards the surface, some of them being highly toxic.

Regarding isotopic signatures ($\delta^{18}O$, $\delta^{2}H$), the ^{2}H enrichment of groundwater (see Fig. 5) can be explained considering the geographical location of the GMTB, and is likely to be related to rainfalls in the Mediterranean areas (Gat and Carmi, 1970, 1987).

Carbon isotopic signatures from DIC ($\delta^{13}C$-DIC) were plotted along with the associated $\delta^{13}C$ values of the related travertine deposits (Fig. 10). In order to establish the possible carbon sources, this figure also shows a clear influence of surficial processes indicated by frequent $\delta^{13}C$ values that correspond to those related to the influence of C3 and C4 plants (O'Leary, 1988), soil CO_2 (Cerling, 1984, 1991) and atmospheric CO_2 (Friedli et al., 1986); and from deep processes (mantle and decarbonation processes). The $\delta^{13}C$-DIC values are relatively constant, caused by the mixture of carbon sources resulting from: (i) carbon sourced by thermal decarbonation or dissolution of marine limestone from the substratum of the basin as well as from soils; and (ii) a minor contribution (0–11%) of probably mantelic CO_2. This last hypothesis is supported on the calculated R/Ra value (0.71) from the free gases sampled in the site (Nisi et al., 2010b; Rodrigo-Naharro et al., 2011, 2012, 2013, Rodrigo-Naharro, 2014) and considering an R/Ra average value of 6.5 for the European mantle (Dunai and Baur, 1995). This situation has been previously described in the Cofrentes area, located 140 km to the NE from the GMTB, where the R/Ra value (0.95) also indicates a small contribution (~12%) of deep-seated (upper mantle) CO_2 (Pérez et al., 1996; Cerón et al., 2000).

Finally, it should be noted that a comprehensive study of this type of groundwater chemistry is important since it is analogous to the groundwater susceptible to host a CO_2-DGS. In this sense, CO_2 would be injected in supercritical state in a CO_2-DGS under these conditions.

5.2. Travertine deposits

The studied travertines are classified as thermogene (Pentecost and Viles, 1994; Pentecost, 1995, 2005; Viles and Pentecost, 2007; Di Benedetto et al., 2011), since they precipitate from warm (20–40 °C) or mesothermal (40–75 °C) groundwater (Renaut and Jones, 2000; Jones

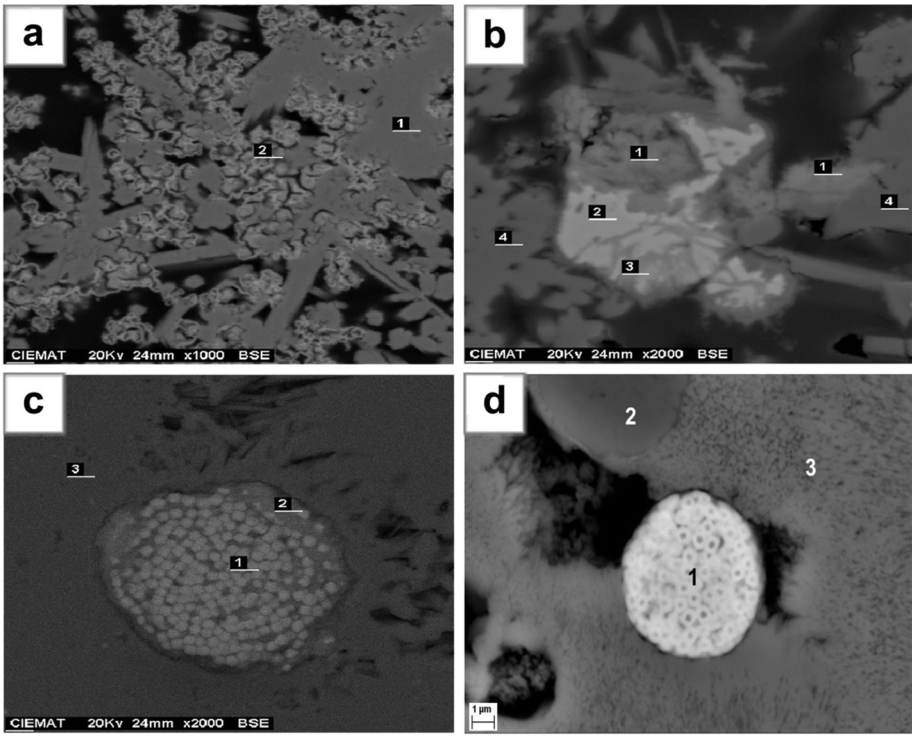

Fig. 9. (a) BEI of botryoidal Fe-oxy-hydroxides (2), probably goethite, filling voids among aragonite needles (1). (b) BEI of a sub-idiomorphic, detrital and partially altered pyrite crystal (3). (c) BEI of a framboidal pyrite (1), surrounded by $CaCO_3$, probably aragonite (3). (d) BEI of a framboidal pyrite totally oxidised (1); quartz (2); $CaCO_3$ (3).

and Renaut, 2010), with higher pCO_2 than in soils, rapid CO_2 degassing and precipitation rates, showing $\delta^{13}C$ values ranging from −3 to 3‰. A very similar example of precipitates in and around active hot springs vent pools, including the groundwater chemistry and the CO_2 source, were studied by Jones and Peng (2016) at Yunnan Province (China). Travertines appear commonly capping faults and joints related to natural and man-induced CO_2 rich springs, and as such they can be used to determine CO_2 leakages.

Concerning the mineralogical composition of these travertines it can be highlighted that they are basically composed of aragonite (El Saladillo and El Reventón) or calcite (El Rincón). Besides this, the aragonite nature of El Saladillo and El Reventón travertines is consistent with the physicochemical features of their corresponding parent waters, since they have almost all the triggering factors for the aragonite precipitation: (i) travertines precipitating from mesothermal waters, with T > 40–45 °C, regardless of water composition (Folk, 1994); (ii) sudden CO_2 degassing of parent waters (Jones and Renaut, 2010); (iii) the presence of high Sr/Mg ratios in the parent waters (Kitano, 1962; Jones and Renaut, 2010); and (iv) the Mg/Ca ratio is > 1, regardless of water T (Folk, 1974). In any case, it seems that T, the Mg/Ca ratio, and/or CO_2-controlled kinetics were the main factors controlling calcite versus aragonite precipitation (De Choudens-Sánchez and González, 2009).

From the petrographic analysis of the samples and the detailed characterisation of the fabrics it can be stated that there is enough evidence indicating that microbes have mediated crystal nucleation in the three studied travertines. The stromatolite-like structures observed indicate that they were formed in a microbial mat environment (Farmer and Des Marais, 1994; Crespo et al., 2013; Rodrigo-Naharro et al., 2013b). Oncoids and stromatolites are common in terrace pools, ponds and on sloping surfaces, where carbonate precipitates upon microbial mats (Renault and Jones, 2000), in which the alternating horizons are attributed to temporal variations in their growth pattern (Folk et al., 1985; Freytet and Verecchia, 1998). Shrubs, which appear in El Saladillo and El Rincón samples, form preferentially in quiescent shallow pools on travertine slopes and are also known to coat grains (Pentecost, 2005). The bacterial shrubs are commonly present and well developed as parts of lake-fill or terraces. Another indicator of the bacterial activity is the H_2S present in all samples (presence of pyrite) that appear to be released from the action of thermophilic bacteria that use oxidised S-compounds as electron acceptors (Renaut and Jones, 2000).

From a chemical point of view, the presence of sulphates in the travertines studied can be explained considering that this anion can replace carbonates in their structures. Similarly, Sr can substitute Ca, particularly in the aragonite structure, though some Sr is related to the presence of celestite, as a neoformed or inherited accessory mineral. Organic CO_2 comes from biological activity, as observed in the petrographic features of the carbonate deposits. In addition, Ba in some samples is related to minor barite contents, whilst As, Zn and U are probably associated with Fe-oxy-hydroxides due to their high geochemical affinity. These geochemical anomalies suggest a cumulative process of these elements during the travertine precipitation. Cerium, La and Zr are related to inherited monazite and zircon detected in the carbonate mass.

Regarding stable isotopes, the $\delta^{13}C$ values were used to discuss the source of CO_2 and any environmental change affecting the carbonate precipitation, since the relationship between temperature and the isotopic fractionation of C in the carbonate-water system is very low. Thus, though $\delta^{13}C$ of carbonates is mainly controlled by the $\delta^{13}C$-DIC when precipitation occurs in equilibrium, this isotopic signature can be modified by any physical (precipitation rate) and/or biological processes occurring in the system before the carbonate precipitation (Shackleton and Opdyke, 1973; Berner, 1997; Kele et al., 2008). Accordingly, the $\delta^{13}C$ range values were plotted along with their corresponding $\delta^{13}C$-DIC (see Fig. 10), which suggests that $\delta^{13}C$ from travertines has an important inorganic origin, although some contribution of organic carbon must be considered. Furthermore, as the isotopic composition of carbonates is enriched in 1 or 2 δ units with respect to $\delta^{13}C$-DIC (Turi, 1986; Romanek et al., 1992), the El Saladillo sample shows the more consistent isotopic signatures since their $\delta^{13}C$ values are ~3‰ more positive than their corresponding DIC. However, the enrichment of ^{13}C in the remaining samples is higher, which could be related to CO_2 degassing processes (Valero-Garcés et al., 1999) or to biological activity (Fouke et al., 2000; Crespo et al., 2013; Rodrigo-

Table 4
Chemical composition of the carbonate deposits.

Elements (wt%)	El Saladillo	El Reventón	El Rincón
CaO	45.17	38.05	41.58
$CO_{2(inorg.)}$	32.04	33.08	40.03
$CO_{2(org.)}$	3.93	3.99	2.89
$Fe_2O_{3(total)}$	13.24	15.55	3.18
SO_3	0.60	2.17	1.08
SrO	0.89	1.28	1.05
SiO_2	1.35	0.01	0.01
Al_2O_3	0.19	0.53	2.52
MgO	0.15	0.38	2.03
MnO	0.00	0.01	1.58
Na_2O	0.45	2.05	0.57
K_2O	0.06	0.11	0.78
TiO_2	0.01	0.01	0.09
P_2O_5	0.04	0.07	0.09
H_2O^-	1.58	2.50	2.00
Total	99.70	99.79	99.48
Trace elements (ppm)			
As	349	305	13
Ba	21	38	200
Zn	50	15	74
U	1.6	2.2	4.6
Ce	4.8	< 3	15
La	15	34	11
Zr	8.7	10	3
Be	20	13	1.1
Co	< 3	< 3	3.8
Cr	< 3	8.0	20
Cu	< 3	< 3	N.D.
Mo	< 3	< 3	1.8
Ni	≤3	< 3	27
Sn	< 3	N.D.	≤0.1
V	< 3	< 3	14
W	≤3	N.D.	1.1
Y	< 3	< 3	4.0
Li	30	44	24
Isotopic signatures** (‰) Trace elements (ppm)			
$\delta^{13}C$	−1.8 ± 0.5	−0.7 ± 0.4	−1.0
$\delta^{18}O$	−11.2 ± 0.5	−8.8 ± 0.3	7.9

*N.D.: Non-Determined.
**The number of analyses was 15 for El Saladillo, 3 for El Reventón and 1 for El Rincón.

Naharro et al., 2013b). In this sense, microorganisms preferentially fix ^{12}C during photosynthesis, causing an enrichment of ^{13}C in the residual DIC and their corresponding carbonates. Therefore, the CO_2 degassing, and at a lesser extent, the organic matter activity, are considered to control the resultant ^{13}C values.

The $\delta^{18}O$ values were determined to establish whether the carbonate deposits precipitated in isotopic equilibrium. The precipitation temperature of these deposits was calculated using the equilibrium equations that relate oxygen ($\delta^{18}O$) isotopic composition and temperature for both aragonite/calcite-water systems. Thus, after a comprehensive review of the specialised literature (Epstein et al., 1953; Craig, 1965; Friedman and O'Neil, 1977; Grossman and Ku, 1986; Patterson et al., 1993; Kim and ÓNeil, 1997; Thorrold et al., 1997; White et al., 1999; Böhm et al., 2000; Owen et al., 2002; Zhou and Zheng, 2003; Kim et al., 2007); the Kim et al. (2007) and Kim and ÓNeil (1997) Eqs. [(1) and (2), respectively] were used considering that the studied carbonates mainly have a continental and inorganic origin.

$$1000\ln\alpha_{(Aragonite-H2O)} = 17.88 \pm 0.13(10^3T^{-1}) - -31.14 \pm 0.46 \quad (1)$$

$$1000\ln\alpha_{(Calcite-H2O)} = 18.03(10^3T^{-1}) - -32.42 \quad (2)$$

where: α is the fractionation factor of aragonite and calcite, respectively; and T is the temperature in K.

The calculated temperature ranges and the measured temperatures of their respective parent waters were listed for comparison (Table 5), showing that the first are lower than the second. Only in El Saladillo were both temperatures very similar. The differences observed can be explained considering either a cooling of the parent waters before carbonate precipitation as waters reach the surface or even during precipitation with a consequent enrichment of ^{18}O. In this sense, Kele et al. (2008) suggested that a correction factor of +8 °C approximately must be applied at the discharge points where fast precipitation rates only cause kinetic isotopic fractionation, as occurs in all the studied sites, except for El Saladillo.

Finally, it is worth mentioning that the importance of the rapid precipitation of travertines is related to the assessment of CO_2 storage performance, since these carbonate deposits could be linked to CO_2 leakages, therefore indicating that the CO_2 storage is jeopardised. Consequently, an anticipatory signal of the bad performance of a CO_2 storage is precisely these deposits, so they can represent effective warnings of possible CO_2 leakages from a CO_2-DGS, taking also into account the very negative $\delta^{13}C$-CO_2 values (~ −30‰) from industrial/anthropogenic activities.

6. Conclusions

Carbonate deposits from the GMTB correspond to travertines considering their fabric and mineralogy, which in turn are aragonitic or calcitic according to the physicochemical factors that characterise the site where they form. Their parent water is CO_2-rich, saline, slightly acid and with the capacity to dissolve, remobilize, transport and deposit heavy elements, some of them toxic. Biological activity promotes the precipitation of travertines as well, as indicated by the appearance of biogenic textural features.

The $\delta^{13}C$ values from both DIC and travertines suggest their origin is mainly inorganic, although a minor organic contribution must be considered in the precipitation of the travertines related to microbial activity. These isotopic signatures could be used as good tracers for the CO_2 escapes from a CO_2-DGS, since the $\delta^{13}C$ value of CO_2 coming from organic fuel combustion is very negative (~-30‰). This isotopic signature could be preserved in spite of the possible CO_2-water–rock interaction processes occurring during the rapid gas escape to the surface through natural (faults) and/or anthropogenic (wells) pathways. Moreover, the difference between measured temperatures of travertine parent waters and calculated temperatures from $\delta^{18}O$ signatures is noticeable, except for the El Saladillo sample. This discrepancy can be partially explained when considering the precipitation rate of travertines that in turn causes kinetic isotopic fractionation and therefore precipitation in disequilibrium.

Groundwater forming aragonite travertines (El Saladillo, El Reventón) contains almost all the triggering factors for the precipitation of this polymorph since this groundwater is mesothermal (T > 40–45 °C), presents high ratios of Sr/Mg and Mg/Ca > 1 and suffering sudden CO_2 degassing as well. In this sense, the identification of these physicochemical features contributes to better identify the underlying and controversial cause of the precipitation of aragonite vs calcite. However, major factors that seem to be controlling the aragonite precipitation in this case cannot be extrapolated, according to the specialized literature, as a general rule for all environments.

Considering the geological setting and based on the geophysical research, the CO_2 being in a supercritical state in certain areas of the aquifer should not be disregarded, which should be hosted at the contact between the Tertiary sediments/volcanic rocks and the Nevado-Filábride materials, and anthropogenically perturbed by geothermal and hydrogeological wells, the latter ones for agricultural purposes. Consequently, the GMTB gathers the main features to be considered as an example of a safe natural CO_2 reservoir in a deep saline aquifer even though its location in an active seismic zone. Thus, there was no evidence of natural CO_2 leakages before the basin was artificially perturbed by the drilling of wells, indicating that a thick marls formation

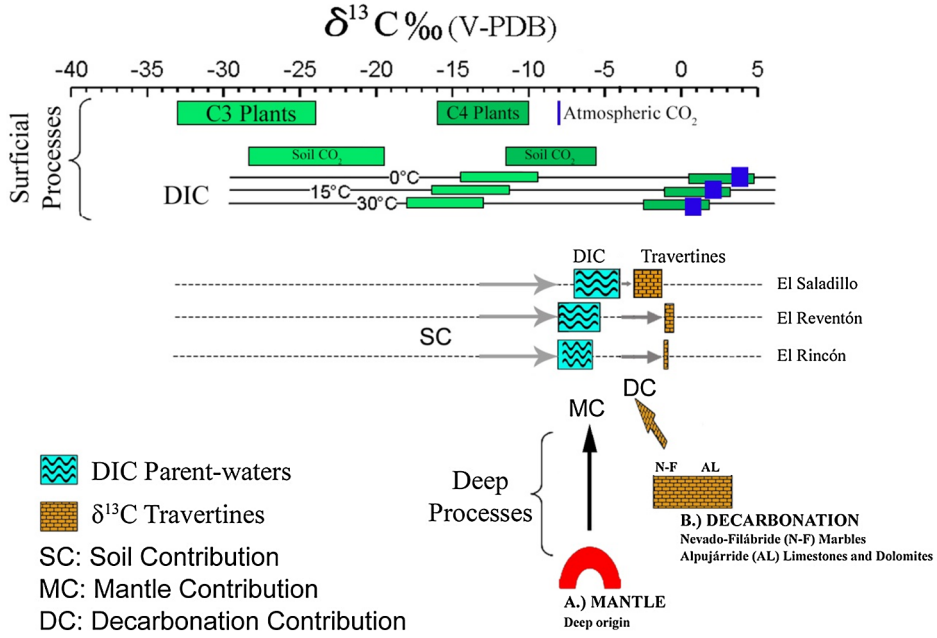

Fig. 10. Graphical representation of the δ^{13}C-DIC values of groundwater and their associated δ^{13}C values of the travertines studied. The more frequent isotopic values for C3 and C4 plants, soil CO_2 and atmospheric CO_2 are represented at the top (Rodrigo-Naharro, 2014).

Table 5
δ^{18}O values of carbonates and their parent waters, calculated temperatures (range and average values) for carbonates, and measured temperatures for their parent waters.

Samples	$\delta^{18}O_{(V\text{-}PDB)}$ (‰) aragonite/calcite [range values]	$\delta^{18}O_{(V\text{-}SMOW)}$ (‰) parent water [range values]	Calculated T (°C) [range values]	Measured parent water T (°C)	Calculated mean T (°C)	Diff.*
El Saladillo	[−12.60, −10.46]	[−7.05, −6.75]	[36.0, 49.5]	45.6	42.8	2.8
El Reventón	[−9.07, −8.47]	[−6.50, −6.04]	[28.0, 34.3]	45.7	31.2	14.5
El Rincón	−7.89	[−7.04, −6.85]	[18.7, 19.5]	35.9	19.1	16.8

* Diff.: Difference between the measured parent water T and the calculated mean T for the travertine precipitation.

filling the basin acted as a very effective seal for the natural CO_2 reservoir. The importance of the rapid precipitation of travertines resides in the warning sign for CO_2 escapes from any CO_2-DGS, indicating either the sealing formation is not impermeable or the existence of CO_2 leakage pathways (wells, fractures, faults, etc.). Furthermore, the use of δ^{13}C values as monitoring tools for CO_2 emissions is very effective to discern the origin of the leaked CO_2.

Finally, it can be argued that the global study of any natural CO_2 reservoir (natural analogue) is a powerful and useful tool to assess the long-term behaviour and safety of a CO_2-DGS. In this sense, the detailed results obtained as well as the methodology used could be applied to any similar geological site selected for the storage of CO_2. This application lies behind the general idea that a comprehensive knowledge of any complex natural system will help us to better predict its potential response.

Declaration of Competing Interest

The authors have no affiliation with any organization with a direct or indirect financial interest in the subject matter discussed in the manuscript.

Acknowledgements

This work was supported by the Spanish Ministry of Science and Innovation and the EU FEDER funds under award number PSE-120000-2008-6. The authors are very grateful to Miguel Ángel Labajo (CIEMAT) for the SEM analyses, and Luis Gutiérrez and Marta Pelayo (CIEMAT) for the XRD analyses. The authors would also like to thank the editor and two anonymous reviewers for their valuable comments and suggestions that greatly contributed to improve the manuscript. Finally, the authors thank Peter M. Booth (Geologist) from Hylton Environmental (UK) for carefully reviewing the text.

References

AGI (American Geological Institute), 1962. Dictionary of geological terms. Garden City N. Y., Dolphin Books (Ed.), pp. 545.
Appelo, C.A.J., Postma, D., 2005. Geochemistry, Groundwater and Pollution, 2nd ed. Balkema Publications, New York.
Araguas-Araguas, L., Díaz-Teijeiro, M.F., 2005. Isotope composition of precipitation and water vapour in the Iberian Peninsula. IAEA-TECDOC-1453, pp. 173–190.
Back, W., Hanshaw, B.B., Plummer, L.N., Rahn, P.H., Rightmire, C.T., Rubin, M., 1983. Process and rate of dedolomitization: mass transfer and ^{14}C dating in a regional carbonate aquifer. Geol. Soc. Am. Bull. 94, 1415–1429.
Ball, J.W., Nordstrom, D.K., 2001. User's manual for WATEQ4F, with revised thermodynamic data base and test cases for calculating speciation of major, trace, and redox elements in natural waters. U.S. Geological Survey Open-File Report, 91–183.
Barnes, I., 1965. Geochemistry of Birch Creek, Inyo County, California a travertine depositing creek in an arid climate. Geochim. Cosmochim. Acta 29, 85–112.
Barnes, I., Irwin, W., White, D., 1978. Global distribution of carbon dioxide discharges and major zones of seismicity. Open-File Report 78-39, US Geological Survey, Washington DC.
Barragán, G., 1997. Algunos datos sobre la actividad hidrotermal pliocena al oeste de Cuevas del Almanzora. Encuadre geológico y cronológico de las manifestaciones magmáticas e hidrotermales de la Depresión de Vera (provincia de Almería). In: García-Rossell, L., Navarro, A. (Eds.), Recursos naturales y medio ambiente en el sureste peninsular. Instituto de Estudios Almerienses, pp. 205–223.
Berner, R.A., 1997. The rise of plants and their effect on weathering and atmospheric CO_2. Science 276, 544–546.
Böhm, F., Joachimski, M.M., Dullo, W.C., Eisenhauer, A., Lehnert, H., Reitner, J., Wörheide, G., 2000. Oxygen isotope fractionation in marine aragonite of coralline

sponges. Geochim. Cosmoch. Acta 64, 1695–1703.
Burnside, N.M., Shipton, Z.K., Dockrill, B., Ellam, R.M., 2013. Man-made versus natural CO_2 leakage: A 400 k.y. history of an analogue for engineered geological storage of CO_2. Geology 41, 471–474.
Cerling, T.E., 1984. The stable isotopic composition of modern sil carbonate and its relationship to climate. Earth Planet. Sci. Lett. 71, 229–240.
Cerling, T.E., 1991. Carbon dioxide in the atmosphere: evidence from Cenozoic and Mesozoic paleosols. Am. J. Sci. 291, 377–400.
Cerón, J.C., Pulido-Bosch, A., 1996. Groundwater problems resulting from CO_2 pollution and overexploitation in Alto Guadalentín aquifer (Murcia, Spain). Environ. Geol. 28, 223–228.
Cerón, J.C., Martín-Vallejo, M., García-Rossell, L., 1998. Geoquímica de las aguas termales con CO_2 del SE de las Cordilleras Béticas. Estudios Geol. 54, 199–207.
Cerón, J.C., Martín-Vallejo, M., García-Rossell, L., 2000. CO_2-rich thermomineral groundwater in the Betic Cordilleras, southeastern Spain: genesis and tectonic implications. Hydrogeol. J. 8, 209–217.
Chafetz, H.S., Meredith, J.C., 1983. Recent travertine pisoliths (pisoids) from southeastern Idaho, USA. In: Peryt, T.M. (Ed.), Coated grains. Springer, Berlin Heidelberg New York, pp. 450–455.
CHS, 2005. Estudio de cuantificación del volumen anual de sobreexplotación de los acuíferos de las unidades hidrogeológicas 07.30 Bajo Guadalentín, 07.32 Mazarrón, 07.25 Santa Yéchar y 07.57 Aledo. Tomos VI, VII y VIII.
Cohn, M., Urey, H.C., 1938. Oxygen exchange reactions of organic compounds and water. J. Am. Chem. Soc. 60, 679–687.
Craig, H., 1961. Isotopic variations in meteoric waters. Science 133, 1702–1703.
Craig, H., 1965. The measurement of oxygen isotope paleotemperatures. In: Tongiorgi, E. (Ed.), Stable Isotopes in Oceanographic Studies and Paleotemperatures. Consiglio Nazionale delle Ricerche, Laboratorio di Geologica Nucleare, Pisa, Spoleto, pp. 161–182.
Crespo, E., Lillo, J., Oyarzun, R., Cubas, P., Leal, M., 2013. The Mazarrón basin, SE Spain: a study of mineralization processes, evolving magmatic series, and geothermal activity. Int. Geol. Rev. 55, 1978–1990.
D'Alessandro, W., Giammanco, S., Bellomo, S., Parello, F., 2007. Geochemistry and mineralogy of travertine deposits of the SW flank of Mt. Etna (Italy): relationships with past volcanic and degassing activity. J. Volcanol. Geotherm. Res. 165, 64–70.
De Choudens-Sánchez, V., González, L.A., 2009. Calcite and aragonite precipitation under controlled instantaneous supersaturation: elucidating the role of $CaCO_3$ saturation state and Mg/Ca ratio on calcium carbonate polymorphism. J. Sediment. Res. 79, 363–376.
Delgado, A., Reyes, E., 2004. Isótopos estables como indicadores paleoclimáticos y paleohidrológicos en medios continentales. Seminarios de la Sociedad Española de Mineralogía. Geoquímica Isotópica Aplicada al Medioambiente 1, 37–53.
Deutsch, W.J., Jenne, E.A., Krupka, K.M., 1982. Solubility equilibria in basalt aquifers: the Columbia Plateau, Eastern Washington, USA. Chem. Geol. 36, 15–34.
Di Benedetto, F., Montegrossi, G., Minissale, A., Pardi, L.A., Romanelli, M., Tassi, F., Delgado-Huertas, A., Pampin, E.M., Vaselli, O., Borrini, D., 2011. Biotic and inorganic control on travertine deposition at Bullicame 3 spring (Viterbo, Italy): a multidisciplinary approach. Geochim. Cosmochim. Acta 75, 4441–4455.
Dunai, T.J., Baur, H., 1995. Helium, neon, and argon systematics of the European subcontinental mantle: implications for its geochemical evolution. Geochim. Cosmochim. Acta 59, 2767–2783.
Epstein, S.Y., Mayeda, T.K., 1953. Variation of the $^{18}O/^{16}O$ ratio in natural waters. Geochim. Cosmochim. Acta 4, 213–224.
Epstein, S., Buchsbaum, R., Lowenstam, H., 1953. Carbonate-water isotopic temperature scale. Geol. Soc. Am. Bull. 62, 417–425.
Farmer, J.D., Des Marais, D.J., 1994. Biological versus inorganic processes in stromatolite morphogenesis: Observations from mineralizing sedimentary systems. In: Stal, L.J., Caumette, P. (Eds.), Microbial Mats: Structure, Development, and Environmental Significance. NATO ASI Series in Ecological Sciences, v. G35. Springer-Verlag, Berlin pp. 61-68.
Fetter, C.W., 1993. Contaminant Hydrogeology. Macmillan Publishing Company, New York, pp. 500.
Folk, R.L., 1974. The natural history of crystalline calcium carbonate: effect of magnesium content and salinity. J. Sediment. Petrol. 44, 40–53.
Folk, R.L., 1994. Interaction between bacteria, nannobacteria, and mineral precipitation in hot springs of central Italy. Géograph. Phys. Quatern. 48, 233–246.
Folk, R.L., Chafetz, H.S., 1983. Pisoliths (pisoids) in quaternary travertines of Tivoli, Italy. In: Peryt, T.M. (Ed.), Coated grains. Springer, Berlin Heidelberg New York, pp. 474–487.
Folk, R.L., Chafetz, H.S., Tiezzi, A., 1985. Bizarre forms of depositional and diagenetic calcite in hot-spring travertines, central Italy. In: Schneidermann, N., Harris, M. (Eds.), Carbonate Cements. SEPM Special Publication, pp. 349–369.
Ford, T.D., Pedley, H.M., 1996. A review of tufa and travertine deposits of the world. Earth-Sci. Rev. 41, 117–175.
Fouke, B.W., Farmer, J.D., Des Marais, D.J., Pratt, L., Sturchio, N.C., Burns, P.C., Discipulo, M.K., 2000. Depositional facies and aqueous–solid geochemistry of travertine depositing hot springs (Angel Terrace, Mammoth Hot Springs, Yellowstone National Park, U.S.A.). J. Sediment. Res. 70, 565–585.
Freytet, P., Verecchia, E.P., 1998. Freshwater organisms that build stromatolites: a synopsis of biocrystallization by prokaryotic and eukaryotic algae. Sedimentology 45, 535–563.
Friedli, H., Lotscher, H., Oeschger, H., Siegenthaler, U., Stauffer, B., 1986. Ice core record of the $^{13}C/^{12}C$ ratio of atmospheric CO_2 in the past two centuries. Nature 324, 237–238.
Friedman, I., 1970. Some investigations of the deposition of travertine from hot springs: I. The isotope chemistry of a travertine-depositing spring. Geochim. Cosmochim. Acta 34, 1303–1315.
Friedman, I., O'Neil, J.R., 1977. Compilation of stable isotope fractionation factors of geochemical interest. Data of Geochemistry. U.S. Geological Survey Professional Paper 440-KK, 6th ed.
Frisia, S., Borsato, A., Fairchild, I.J., McDermott, F., 2000. Calcite fabrics, growth mechanisms, and environments of formation in speleothems from the Italian Alps and Southwestern Ireland. J. Sediment. Res. 70, 1183–1196.
Gal, F., Michel, B., Gilles, B., Frédéric, J., Karine, M., 2011. CO_2 escapes in the Laachersee region, East Eifel, Germany: application of natural analogue onshore and offshore geochemical monitoring. Int. J. Greenhouse Gas Control 5, 1099–1118.
Gat, J.R., Carmi, I., 1970. Evolution in the isotopic composition of atmospheric waters in the Mediterranean Sea area. J. Geophys. Res. 75, 3039–3048.
Gat, J.R., Carmi, I., 1987. Effect of climate changes on the precipitation patterns and isotopic composition of water in a climate transition zone: case of the Eastern Mediterranean Sea area. The Influence of Climate Change and Climatic Variability on the Hydrologic Regime and Water Resources. Proceedings of the Vancouver Symposium. No. 168. IAHS Publ., pp. 513–523.
Gibert, R.O., Taberner, C., Sáez, A., Giralt, S., Alonso, R.N., Edwards, R.L., Pueyo, J.J., 2009. Igneous origin of CO_2 in ancient and recent hot-spring waters and travertines from the Northern Argentinean Andes. J. Sediment. Res. 79, 554–567.
Gómez-Pugnaire, M.T., Torres-Ruiz, J., Martínez Martínez, J.M., 1981. Escapolita en rocas de las series Permo-Triásicas del Complejo Nevado-Filábride (Cordilleras Béticas) Origen. Boletín de la Sociedad Española de Mineralogía IV, 37–46.
Grossman, E.L., Ku, T.-L., 1986. Oxygen and carbon isotope fractionation in biogenic aragonite: temperature effects. Chem. Geol. 59, 59–74.
Guo, L., Riding, R., 1998. Hot-spring travertine facies and sequences, Late Pleistocene, Rapolano Terme, Italy. Sedimentology 45, 163–180.
Guo, L., Riding, R., 1999. Rapid facies changes in Holocene fissure ridge hot spring travertines, Rapolano Terme, Italy. Sedimentology 46, 1145–1158.
Herrero, M.J., Escavy, J.I., 2010. Economic aspects of continental carbonates and carbonates transformed under continental conditions. In: Alonso-Zarza, A.M., Tanner, L. H. (Eds.), Carbonates in Continental Settings: Geochemistry, Diagenesis and Applications. Developments in Sedimentology 62, pp. 275-296.
IGME, 1979. La problemática de las aguas en el término municipal de Totana (Murcia), pp. 26.
IGME, 1981. Los recursos hídricos subterráneos de la Comarca Mazarrón-Águilas. Situación actual y perspectivas futuras, 4 tomos.
IGME-ADARO, 1985. Investigación de las posibilidades de existencia de energía geotérmica en la comarca de Mazarrón-Águilas (Murcia). Informe interno, VIII Tomos.
Jones, B., Renaut, R.W., 1996. Morphology and growth of aragonite crystals in hot-spring travertines at Lake Bogoria, Kenya Rift Valley. Sedimentology 43, 323–340.
Jones, B., Peng, X., 2016. Mineralogical, crystallographic, and isotopic constraints on the precipitation of aragonite and calcite at Shiqiang and other hot springs in Yunnan Province, China. Sediment. Geol. 345, 103–125.
Jones, B., Renaut, R.W., 2010. Calcareous spring deposits in continental settings. In: Alonso-Zarza, A.M., Tanner, L.H. (Eds.), Carbonates in Continental Settings: Facies, Environments, and Processes. Developments in Sedimentology 61, pp. 177-224.
Kele, S., Demény, A., Siklósy, Z., Németh, T., Tóth, M., Kovács, M.B., 2008. Chemical and stable isotope composition of recent hot-water travertines and associated thermal waters, from Egerszalók, Hungary: depositional facies and non-equilibrium fractionation. Sedim. Geol. 211, 53–72.
Kim, S.T., ÓNeil, J.R., 1997. Equilibrium and nonequilibrium oxygen isotope effects in synthetic carbonates. Geochim. Cosmochim. Acta 61, 3461–3475.
Kim, S.T., ÓNeil, J.R., Hillarie-Marcel, C., Mucci, A., 2007. Oxygen isotope fractionation between synthetic aragonite and water: influence of temperature and Mg^{2+} concentration. Geochim. Cosmochim. Acta 71, 4704–4715.
Kitano, Y., 1962. A study of the polymorphic formation of calcium carbonate in thermal springs with an emphasis on the effect of temperature. Bull. Chem. Soc. Japan 35, 1980–1985.
Liu, Z., Zhang, M., Li, Q., You, S., 2003. Hydrochemical and isotope characteristics of spring water and travertine in the Baishuitai area (SW China) and their meaning for paleoenvironmental reconstruction. Environ. Geol. 44, 698–704.
Martín-Vallejo, M., 1997. . El sistema hidrotermal de la Cuenca del río Almanzora, N de la provincia de Almería. (The hydrothermal system of the Almanzora river basin, N of Almería province). PhD thesis. University of Granada, Spain. Published thesis.
Minissale, A., Kerrich, D.M., Magro, G., Murrell, M.T., Paladini, M., Rihs, S., Sturchio, N.C., Tassi, F., Vaselli, O., 2002. Structural, hydrological, chemical and climatic parameters affecting the precipitation of travertines in the Quaternary along the Tiber valley, north of Rome (Italy). Earth Planet. Sci. Lett. 203, 709–728.
Moore, G.W., 1956. Aragonite speleothems as indicators of paleotemperature. Am. J. Sci. 254, 746–753.
Moore, J., Adams, M., Allis, R., Lutz, S., Rauzi, S., 2003. CO2 mobility in natural reservoirs beneath the Colorado Plateau and Southern Rocky Mountains: an example from the Springerville–St Johns Field, Arizona and New Mexico. Proceedings of the Second Annual Conference on Carbon Sequestration, 5–8 May, Alexandria VA.
Moreno, L., De la Losa, A., 2008. INAQUAS: Utilidad para la interpretación de análisis químicos de aguas subterráneas. Publicaciones del IGME pp. 14.
Navarro, A., Fernández-Uría, A., Doblas, J.G., 1993. Las aguas subterráneas en España: Estudio de síntesis. Instituto Tecnológico Geominero de España, Madrid, España.
Nemeth, K., 1963. Photometric determination of sulphate in soil extracts. Zeitschrift für Pflanzenernährung, Düngung, Bodenkunde 103, 193–196.
Nisi, B., Vaselli, O., Tassi, F., Gimeno, M.J., Acero, P., Poreda, R.J., Rodrigo-Naharro, J., Delgado, A., Pérez del Villar, L., 2010a. Effects of deep saline CO2-rich waters in the shallow aquifers from the Mazarrón-Gañuelas Tertiary basin (central-southern Spain). Proceedings of the 85° Congresso Nazionale; 2010 Sep 6-8, Pisa, Italy. Società

Geologica Italiana; 2010. Rendiconti Online della Società Geologica Italiana 11, 186-187.
Nisi, B., Vaselli, O., Tassi, F., Gimeno, M. J., Acero, P., Poreda, R. J., Rodrigo-Naharro, J., Delgado, A., Pérez del Villar, L., 2010b. Water deterioration of the Mazarrón-Gañuelas aquifer (SE Spain) by deep-seated CO2 saline-waters as evidenced by geochemical and isotopic investigation. Proceedings of the 89th SIMP Meeting; 2010 Sep 13-15, Ferrara, Italy. Societá Italiana di Mineralogia e Petrologia; 2010, S2.2-O3.
Nordstrom, D.K., Ball, J.W., 1989. Mineral saturation states in natural waters and their sensitivity to thermodynamic and analytic errors. Sci. Geol. Bull. 42, 269–280.
O'Leary, M.H., 1988. Carbon isotopes in photosynthesis. BioScience 38, 328–336.
Owen, R., Kennedy, H., Richardson, C., 2002. Experimental investigation into partitioning of stable isotopes between scallop (Pecten maximus) shell calcite and sea water. Palaeogeogr. Palaeoclimatol. Palaeoecol. 185, 163–174.
Parkhurst, D.L., Appelo, C.A.J., 2013. Description of input and examples for PHREEQC Version 3 — A computer program for speciation, batch-reaction, one-dimensional transport, and inverse geochemical calculations. US Geological Survey Techniques and Methods, book 6, chap A43, pp. 497.
Patterson, W.P., Smith, G.R., Lohmann, K.C., 1993. Continental paleothermometry and seasonality using the isotopic composition of aragonitic otoliths of freshwater fishes. Geophys. Monogr. Ser. 78, 191–202.
Pentecost, A., 1995. The Quaternary travertine deposits of Europe and Asia Minor. Quarter. Sci. Rev. 14, 1005–1028.
Pentecost, A., 2005. Travertine. Springer, Berlin, pp. 445.
Pentecost, A., Viles, H., 1994. A review and reassessment of travertine classification. Géograp. Phys. Quatern. 48, 305–314.
Pérez, N.M., Nakai, S., Wakita, H., Beltrán, A., Redondo, R., 1996. Preliminary results on $^{3}He/^{4}He$ isotopic ratios in terrestrial fluids from Iberian Peninsula: seismotectonic and neotectonic implications. Geogaceta 20, 830–833.
Pérez del Villar, L., Pelayo, M., Prado-Pérez, A.J., Recreo, F., Vilanova, E., Grandia, F., Duro. L., Domènech, C., Martell, M., Delgado, A., Auqué, L.F., Gimeno, M.J., Acero, P., 2008. Almacenamiento geológico de CO2: análogos naturales del almacenamiento y escape. Fundamentos, ejemplos y aplicaciones para la predicción de riesgos y la evaluación del comportamiento a largo plazo. Comunicación técnica. 9° Congreso Nacional del Medio Ambiente, Madrid. Available at http://www.conama9.conama.org/conama9/download/files/CTs/2689_LP%E9rez.pdf (accessed 8 January 2019).
Plummer, L., Busenberg, N.E., 1982. The solubilities of calcite, aragonite and vaterite in CO_2 – H_2O solutions between 0 and 90°C, and an evaluation of the aqueous model for the system $CaCO_3$ – CO_2 – H_2O. Geochim. Cosmochim. Acta 46, 1011–1040.
Prado-Pérez, A.J., Pérez del Villar, L., 2011. Dedolomitization as an analogue process for assessing the long-term behaviour of a CO_2 deep geological storage: the Alicún de las Torres thermal system (Betic Cordillera, Spain). Chem. Geol. 289, 98–113.
Prado-Pérez, A.J., Delgado Huertas, A., Crespo, M.T., Martín Sánchez, A., Pérez del Villar, L., 2013. Late Pleistocene and Holocene paleoclimatic and palaeoenvironmental reconstruction at middle geographical latitude: an approach based on the isotopic record from a travertine formation in the Guadix-Baza basin, Spain. Geol. Magaz. 150, 602–625.
Priewisch, A., Crossey, L.J., Karlstrom, K.E., McPherson, B.J., Mozley, P., 2013. Ancient and modern sites of natural CO2 leakage: Geochemistry and geochronology of Quaternary and modern travertine deposits on the Colorado Plateau, USA, and implications for CO2 sequestration. American Geophysical Union, Fall Meeting 2013, abstract #V41A-2777.
Renaut, R.W., Jones, B., 2000. Microbial precipitates around continental hot springs and geysers. In: Riding, R.E., Awramik, S.M. (Eds.), Microbial Sediments. Springer, Berlin, pp. 187–195.
Rodrigo-Naharro, J., 2014. El análogo natural de almacenamiento y escape de CO_2 de la cuenca de Gañuelas-Mazarrón: implicaciones para el comportamiento y la seguridad de un almacenamiento de CO_2 en estado supercrítico. Universidad Politécnica de Madrid PhD thesis pp. 427. Published thesis. ISBN: 978-84-7834-738-4.
Rodrigo-Naharro, J., Vaselli, O., Tassi, F., Clemente-Jul, C., Pérez del Villar, L., 2011. Effects on the shallow aquifers by CO2 leakages in a tertiary basin (province of Murcia, Spain). Fifth International Conference on Clean Coal Technologies CCT2011, Zaragoza (Spain).
Rodrigo-Naharro, J., Nisi, B., Vaselli, O., Quindós, L.S., Pérez del Villar, L., 2012. Measurements and relationships between CO_2 and ^{222}Rn in a natural analogue for CO_2 storage and leakage: the Mazarrón Tertiary Basin (Murcia, Spain). Geo-Temas 13, 1978–1981.
Rodrigo-Naharro, J., Nisi, B., Vaselli, O., Lelli, M., Saldaña, R., Clemente-Jul, C., Pérez del Villar, L., 2013a. Diffuse soil CO_2 flux to assess the reliability of CO_2 storage in the Mazarrón-Gañuelas Tertiary Basin (Spain). Fuel 114, 162–171.
Rodrigo-Naharro, J., Delgado, A., Herrero, M.J., Granados, A., Pérez del Villar, L. 2013b. Current travertines precipitation from CO2-rich groundwaters as an alert of CO2 leakages from a natural CO2 storage at Gañuelas-Mazarrón Tertiary Basin (Murcia, Spain). Informe Técnico CIEMAT 1279, 54 pp. ISSN: 1135-9420.
Rodrigo-Naharro, J., Quindós, L.S., Clemente-Jul, C., Mohamud, A.H., Pérez del Villar, L., 2017. CO_2 degassing from a Spanish natural analogue for CO_2 storage and leakage: Implications on ^{222}Rn mobility. Appl. Geochem. 84, 297–305.
Rodrigo-Naharro, J., Aracil, E., Pérez del Villar, L., 2018. Geophysical investigations in the Gañuelas-Mazarrón Tertiary basin (SE Spain): a natural analogue of a geological CO_2 storage affected by anthropogenic leakages. J. Appl. Geophys. 155, 187–198.
Romanek, C.S., Grossman, E.L., Morse, J.W., 1992. Carbon isotopic fractionation in synthetic aragonite and calcite: effects of temperature and precipitation rate. Geochim. Cosmochim. Acta 56, 419–430.
Sanz De Galdeano, C., Vera, J.A., 1992. Stratigraphic record and palaeogeographical context of the Neogene basins in the Betic Cordillera. Spain. Basin Res. 4, 21–36.
Schütze, C., Sauer, U., Beyer, K., Lamert, H., Bräuer, K., Strauch, G., Flechsig, C., Kämpf, H., Dietrich, P., 2012. Natural analogues: a potential approach for developing reliable monitoring methods to understand subsurface CO_2 migration processes. Environ. Earth Sci. 67, 411–423.
Shackleton, N.J., Opdyke, N.D., 1973. Oxygen isotope and palaeomagnetic stratigraphy of equatorial Pacific core V28–238: Oxygen isotope temperatures and ice volumes on a 10^5 and 10^6 year scale. Quat. Res. 3, 39–55.
Sharp, Z.D., Atudorei, V., Durakiewicz, T., 2001. A rapid method for determination of hydrogen and oxygen isotope ratios from water and hydrous minerals. Chem. Geol. 178, 197–210.
Shipton, Z.K., Evans, J.P., Kirchner, D., Kolesar, P.T., Williams, A.P., Heath, J., 2004. Analysis of CO_2 leakage through "low-permeability" faults from natural reservoirs in the Colorado Plateau, southern Utah. In: Baines, S.J., Worden, R.H. (Eds.), Geological Storage of Carbon Dioxide. Geological Society, London, Special Publications, pp. 43–58.
Tena, J.M., Auqué, L.F., Gimeno, M.J., Fernández, J., Mandado, J., 1990. El equilibrio cuarzo/solución de 0 a 100° C. Variaciones en el cálculo de K según los calibrados geotermométricos y las funciones de T utilizadas en programas de modelización geoquímica. Estudios Geológicos 46, 15–24.
Thorrold, S.R., Campana, S.E., Jones, C.M., Swart, P.K., 1997. Factors determining $\delta^{13}C$ and $\delta^{18}O$ fractionation in aragonitic otoliths of marine fish. Geochim. Cosmochim. Acta 61, 2909–2919.
Torres-Ruiz, J., 1980. Los yacimientos de hierro de la comarca del Marquesado del Zenete: Alquife y las Piletas (Granada, Cordillera Bética). Universidad de Granada, Spain, pp. 312 PhD thesis Published thesis.
Turi, B., 1986. Stable isotope geochemistry of travertines. In: Fritz, P., Fontes, J.C. (Eds.), Handbook of Environmental Isotope Geochemistry. Elsevier, Amsterdam, pp. 207–238.
USEPA, 2012. 2012 Edition of the Drinking Water Standards and Health Advisories. EPA 822-S-12-001, pp. 20.
Uysal, I.T., Feng, Y.-X., Zhao, J.-X., Isik, V., Nuriel, P., Golding, S.D., 2009. Hydrothermal CO_2 degassing in seismically active zones during the late Quaternary. Chem. Geol. 263, 442–454.
Valero-Garcés, B.L., Delgado-Huertas, A., Ratto, N., Navas, A., Machin, J., 1999. Large ^{13}C enrichment in primary carbonates from Andean Altiplano lakes, Northwest Argentina. Earth Planet. Sci. Lett. 171, 253–266.
Viles, H.A., Pentecost, A., 2007. Tufa and travertine. In: Nash, D.J., McLaren, S.J. (Eds.), Geochemical Sediments and Landscapes. Wiley-Blackwell, Oxford, pp. 173–199.
White, R.M.P., Dennis, P.F., Atkinson, T.C., 1999. Experimental calibration and field investigation of the oxygen isotopic fractionation between biogenic aragonite and water. Rapid Commun. Mass Spectrom. 13, 1242–1247.
Zhou, G.T., Zheng, Y.F., 2003. An experimental study of oxygen isotope fractionation between inorganically precipitated aragonite and water at low temperatures. Geochim. Cosmochim. Acta 67, 387–399.
Zhu, C., Anderson, G., 2002. Environmental applications of geochemical modeling. Cambridge University Press pp. 284.